

Article

Development of coffee biochar filler for the production of electrical conductive reinforced plastic

Mauro Giorcelli *, Mattia Bartoli

Affiliation: Politecnico di Torino, C.so Duca degli Abruzzi 24, 10129 Torino;

* mauro.giorcelli@polito.it, +390110904327 (M.G.)

Abstract: In this work we produced biochar by coffee waste and use it as filler in epoxy resin composite with the aim to increase their electrical properties. The biochar and biochar based composite electrical conductivity were studied in function of applied pressure and compared with carbon black and carbon black composite. The applied pressure has the aim to investigate the behaviour of filler in powder or dispersed in composite in function of compression. Results showed that even if the coffee biochar has less conductivity if compared with carbon black in powder form, it has better conductivity in composite if compared with carbon black. Composite mechanical properties were tested and they are generally improved respect to neat epoxy resin.

Keywords: Electrical properties, Mechanical properties, Recycling, Epoxy resin

1. Introduction

Anthropogenic waste streams management is one of the unresolved main problem of the industrialized societies[1,2]. As recently reported by Christoph Sanger [3], the worldwide coffee production had been 159.7 million of bags in crop year 2017/18 (about 9.6 Mtons). With a mean of 5 kg/capita per year in the traditional markets (Germany, Italy, France, USA and Japan) and an increasing consumption in the emerging markets (South Korea, Russia, Turkey and China), coffee waste stream has risen a relevant problem not only after consumption but also during wet processing of coffee beans when 1 ton of fresh berry results in about 400 Kg of wet waste pulp. Several solutions have been proposed such as the production of biogas[4] and flavours [5], use as filler in ceramics construction[6] or as absorbent for the removal of basic dyes from aqueous solutions[7]. Also, coffee wastes have been used as feedstock for pyrolytic conversion producing hydrogen rich gas[8] and fuel quality biochar[9]. Biochar has been used not only as sold fuel but also as high performance material [10,11] for electrochemical[12] and energy storage applications[13], and for composites production[14-16].

In the realm of polymer composites, carbon black (CB) plays the main role especially in the automotive field with an estimated consumption of 8.1 Mton/year according with data released by International carbon black association [17]. CB has been used for producing conductive composites[18] but, as recently reported by Quosai et al.[19], coffee based biochar also showed remarkably conductive properties. Furthermore, coffee biochar production is based on using a food waste stream while oil based feedstock is required for CB production decreasing the environmentally impact of the production process [20-22].

Among different polymers, in this work we investigated epoxy resins doped with carbon fillers. As well known, epoxy resin is a thermoset polymer widely applied in the field of coatings[23], adhesives[24], casting[25], potting[26], composites[27], laminates[28] and encapsulation of semiconductor devices[29]. Epoxy resins are intensively used because their peculiar properties such as high strength, good stiffness, good thermal stability, excellent heat, moisture and chemical resistance[30,31].

Conductive epoxy resin is an interesting material because its versatility in different large scale application fields such as coatings and adhesives. In these large scale applications, the filler cost is a crucial issue. High cost carbon fillers such as carbon nanotubes and graphene induce in the host

polymer matrix an increment of its electrical and mechanical properties[32-35] but are not a suitable choice for industrial scale production. This is mainly due to the high cost, up to 300 k\$/Kg[36], and problems correlated to low productivity of the plants are well known[37]. Thus, low cost carbon fillers, such as CB, but not derived from fossil fuels are a topic of relevant interest.

Therefore, in this study, we investigated the possibility to use biochar derived from pyrolytic conversion of coffee waste stream, as innovative carbon filler to produce conductive epoxy based composites. Results were compared with CB based composites. Electrical and mechanical properties are investigated.

2. Materials and Methods

2.1 Carbonaceous materials preparation and characterization

Exhausted coffee powder was selected as a real case study. It has been collected from Bar Katia (Turin, Italy) supplied by Vergnano (Arabica mixture). Coffee was collected and dried at 105°C for 72h. Coffee samples (100g) were pyrolyzed using a vertical furnace and a quartz reactor, heating rate of 15°C/min and kept at the final temperature (400, 600, 800 and 1000°C) for 30 min. Samples will be shorten as C400, C600, C800 and C1000 respectively. Biochar was grinded using a mechanical mixer (Savatec BB90E) for 10 minutes in order to decrease the particle size. Commercial CB (VULCAN® 9 N115) has been used to compare with coffee biochar.

Ash contents of coffee and carbon based materials (biochars, and carbon black) were evaluated using a static furnace set at 550°C or 800°C respectively for 6h.

All samples have been investigated from morphological point of view using a Field Emission Scanning Electrical microscopy (FE-SEM, Zeis SupraTM 40).

Particle size distribution of carbon fillers has been evaluated using a laser granulometry (Fritsch Analysette 22, Idar-Oberstein, Germany) after dispersion in ethanol and sonication in an ultrasonic bath for 10 minutes.

Coffee, biochars and carbon black were analysed through FT-IR (Nicolet 5700, Thermoscientific) on ATR mode (Smartorbit, Thermoscientific) in the range from 500 cm⁻¹ to 4000 cm⁻¹.

Biochars and carbon black were analysed through Raman spectroscopy using Renishaw® Ramanscope InVia (H43662 model).

2.2 Composites preparation

Biochar, derived from coffee, and commercial carbon black containing epoxy composites were produced using a two component BFA diglycidyl resin (CORES epoxy resin, LPL). Carbonaceous filler (15 wt.%) were dispersed into epoxy monomer using a tip ultrasonicator apparatus (Sonics Vibra-cell) for 15 min. After the addition of curing agent, the mixture was ultrasonicated for other 2 min and left into the moulds for 16 h at room temperature. A final thermal curing was performed using a ventilated oven (I.S.C.O. Srl "The scientific manufacturer") at 70°C for 6h.

2.3 Electrical characterization

The measurement set-up was derived from [15] and is sketched in Figure 1a for fillers and Figure 1b for composites. The instrument is composed of two solid copper cylinders, 30 mm in diameter and 5 cm in length, encapsulated in a hollow Plexiglas cylinder with a nominal inner diameter of 30 mm in the case of filler electrical characterization. In this configuration, the inner diameter is slightly higher so that it is possible to force the copper rods inside the Plexiglas cavity and the upper rod can slide inside the cylinder during the measurement. This arrangement creates an internal chamber between the two cylinders, where the carbon powder can be inserted. In case of composite the Plexiglas cylinder was removed and the sample was positioned between the aligned copper cylinders. The electrical resistance of the powders or composite was measured at increasing loads (up to 1400 bar) applied by a hydraulic press (Specac Atlas Manual Hydraulic Press 15T). Electrically insulating sheets were placed between the conductive cylinders and the load surfaces in order to ensure that the electrical signal pass through the sample. The resistance of the carbon fillers was measured using an Agilent 34401A multimeter.

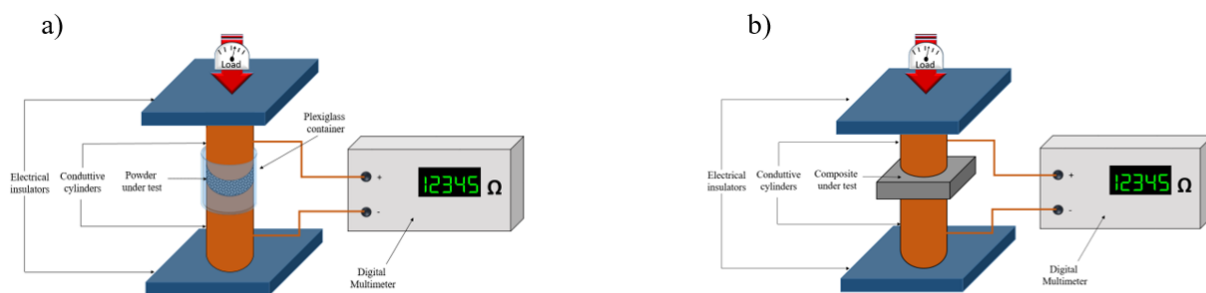


Figure 1. Sketch of Measurement set-up for conductivity study of a) carbon fillers and b) composite.

2.4 Composite mechanical characterization

Carbonaceous materials containing composites were produced as dog-bones shaped according with ASTM 638 procedure. Samples were tested using a MSTS machine (MTS Q-test10). Data were analysed using a self-developed software compiled using Matlab.

3. Results

3.1. Carbonaceous materials characterization

Ash content of feedstock and carbonaceous materials were preliminary investigated and summarized in Figure 2.

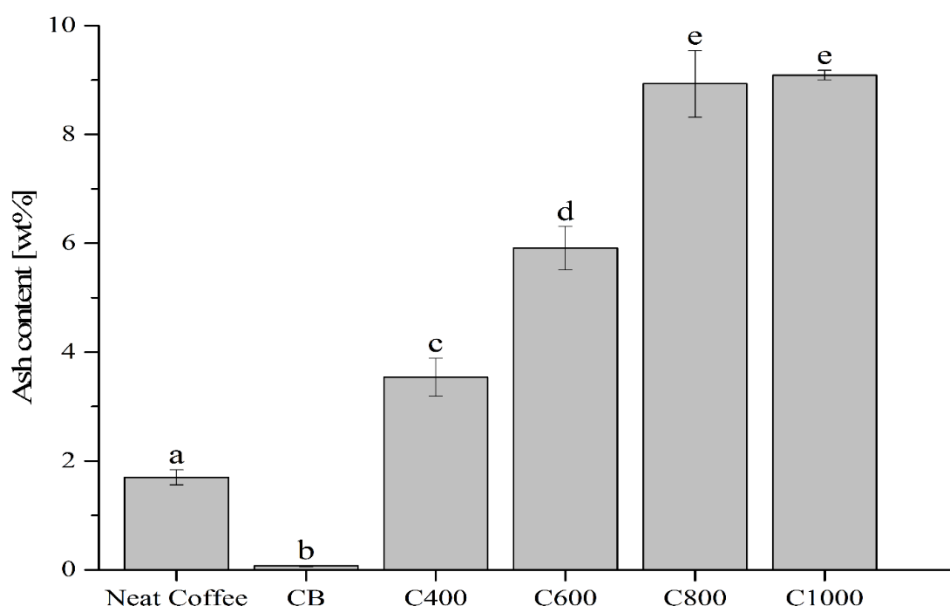


Figure 2. Ash contents of neat coffee, CB, C400, C 600, C800, C1000. Columns marked with different letters are significantly different ($p < 0.05$).

The ash content of neat coffee was 1.70 ± 0.14 wt.% and it increased with temperature increments reaching value around 9 wt.% in the case of C800 (8.92 ± 0.61 wt.%) and C1000 (9.09 ± 0.09 wt.%). CB showed a very low ash content (0.07 ± 0.01 wt.%) according to Medalia et al.[38] mainly as oxides. Ash content increment at higher temperatures was imputable to advance pyrolytic degradation of the organic matrix leading to the concentration of inorganic residue [39] that did not underwent to any temperature induced degradation. Ash content in CB is marginal as expected.

The effect of pyrolytic temperature on biochar morphology was studied using FE-SEM as shown in Figure 3. Neat coffee showed a flaked collapsed structures (Figure 3 a-b) than was retained by C400 after pyrolysis at 400°C (Figure 3 e-f). Increasing temperature to 600°C lead to the formation of porous structures with average diameters close to 30 μm separated by carbon lamellae with a thickness around 1 μm (Figure 3 g-h). At 800 °C, biochar recovered lost the structure cause to the massively release of volatile organic matters during the overall pyrolytic process that induced the collapse of carbonaceous structures together with and improved grindability[40]. At 1000°C, the increased temperature allowed the massively formation of carbon-carbon bonds that promoted the stabilization of porous architecture with nanoscale lamellae structures. CB showed a typical highly aggregate spherule based shape with average diameter of single particles around 50 nm.

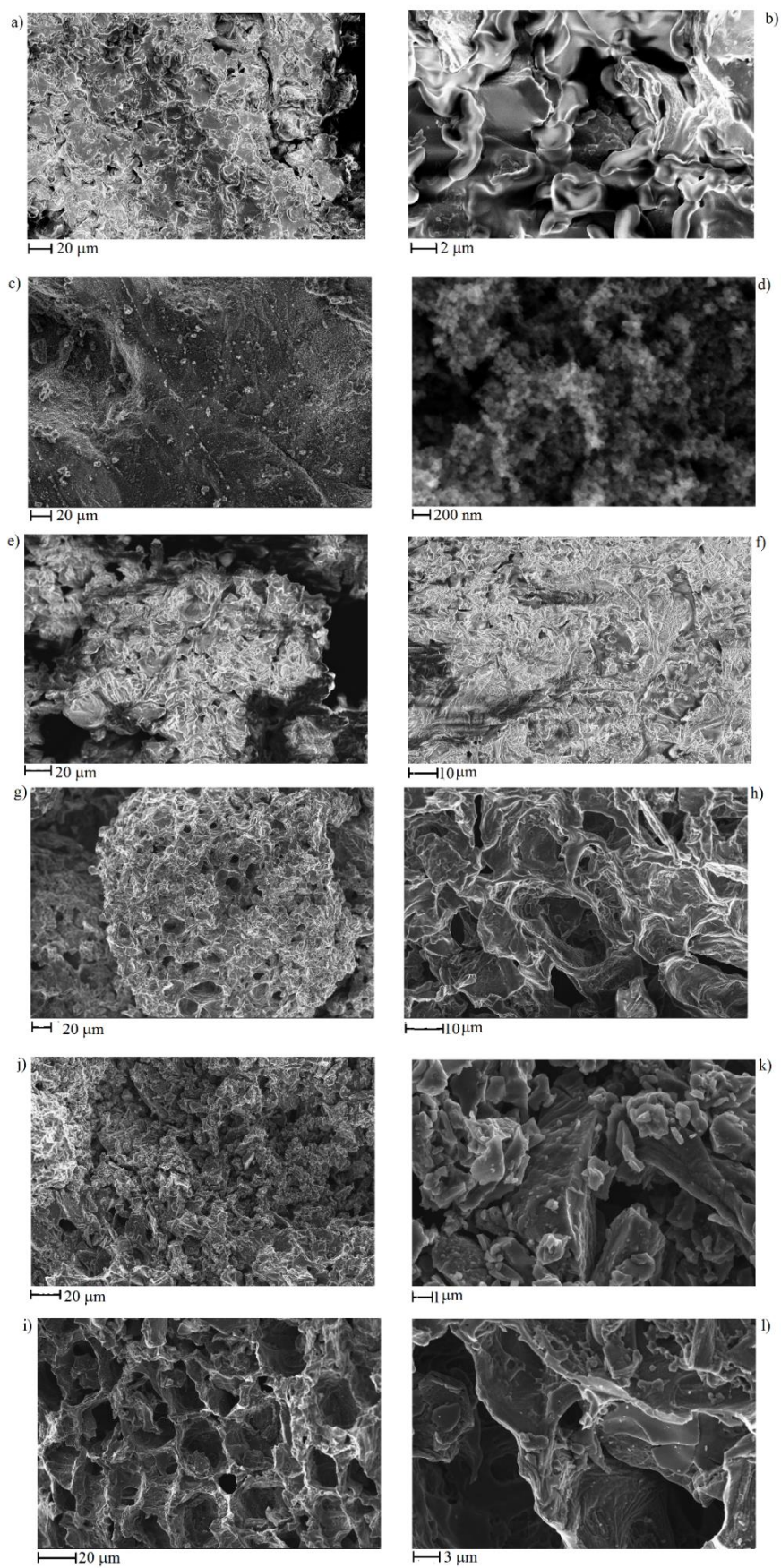


Figure 3. FE-SEM captures of a-b) neat coffee, c-d) CB, e-f) C400, g-h) C600, j-k) C800 and i-l) C1000°C.

Organic component of significant carbonaceous materials was also analysed using both FT-IR and Raman spectrometry techniques. Among carbonaceous materials, we reported neat coffee, C1000 and CB. Results are reported in Figure 4.

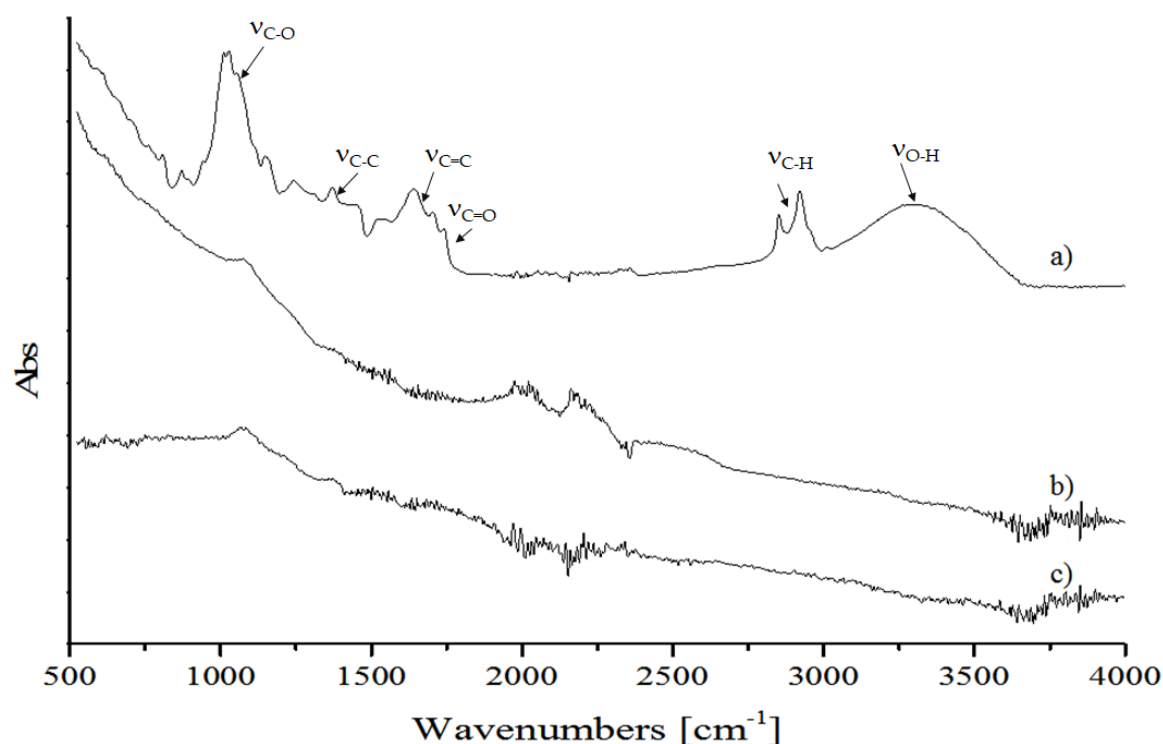


Figure 4: FT-IR spectra (ATR mode) of a) neat coffee, b) coffee biochar produced at 1000°C and c) carbon black in the range of 500-4000 cm^{-1} .

FT-IR spectrum of neat coffee showed the broad band of $\nu_{\text{O-H}}$ (3300-3500 cm^{-1}), the bands of saturated $\nu_{\text{C-H}}$ (2850-2950 cm^{-1}), $\nu_{\text{C=O}}$ (1710-1741 cm^{-1}) due to the carboxylic functionalities, $\nu_{\text{C=C}}$ (1540-1638 cm^{-1}) due to the presence of aromatic structures, saturated and unsaturated $\delta_{\text{C-H}}$ (1370-1440 cm^{-1}), saturated $\nu_{\text{C-C}}$ (1243 cm^{-1}), $\nu_{\text{C-O}}$ (1030-1148 cm^{-1}) and out-of-plane $\delta_{\text{O-H}}$ below 700 cm^{-1} . Those bands clearly identified a lignocellulosic derived matrix with massively presence of polysaccharides and aromatics. C1000 did not show any of the characteristic bands of organic matrix but show an enveloped of bands below 1800 cm^{-1} due to carbon skeletal movements. Contrary, CB showed low bands intensity below 1000 cm^{-1} due the lower variety of carbon structure embedded into particles.

Raman spectra normalized on G peak are showed in Figure 5. Coffee biochars have the typical profiles of amorphous materials[41] while CB is more graphitic. The graphitic structure for CB could be observed by the deep gorge between D and G peaks and their shaped structure. The increasing of $I_{\text{D}}/I_{\text{G}}$ ratio for biochars moving from a pyrolytic temperature of 400°C to 1000°C, is evident. This increasing of $I_{\text{D}}/I_{\text{G}}$ ratio could be ascribed to the progressively loss of residual functional groups with the increase of temperature. This observation was also supported by the decrease of fluorescence[42]. Due to the loss of less intense part of these weak interactions biochar underwent to an appreciable disorganization together with aromatic structure formation, in particular up to 600°C, without the completion of a proper graphitization process that occurs at higher temperature [43].

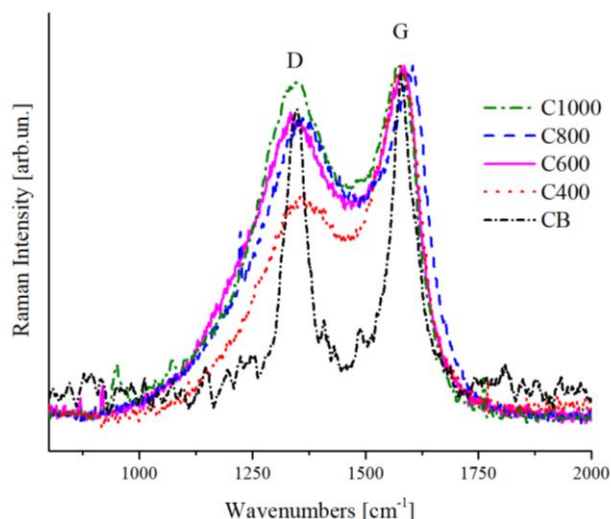


Figure 5: Magnification of Raman spectra in the range from 800 cm^{-1} to 2000 cm^{-1} of C400, C600, C800, C1000 and CB

3.2 Composite characterization

3.2.1 Electrical characterization of carbonaceous filler and composites

The set up showed in figure 1a was used for biochar powders electrical characterization. Around 3 grams of carbonaceous powder, able to create a few millimetres distance between copper cylinders was positioned in the chamber. After the closure of the chamber a pressure was applied with the aim to compact the powder. The pressure range was from 0 to 1500 bar (step of 250 bar). For each step the stabilized value of resistivity was registered such as the distance between the copper cylinders. The same procedure was repeated for composite of few millimetre thickness. Carbonaceous powders and composite decrease their resistance value during compression till reach a plateau when high pressure was reached. The decreasing of resistance value could be correlated with the decreasing of space between carbon particles as sketched in Figure 6. In the case of powders, the void among particles collapse with a production of compact carbon agglomerate as showed in Figure 6a. In the case of composite, Figure 6b shows the mechanism where the polymer chains flows let the carbon particles put near.

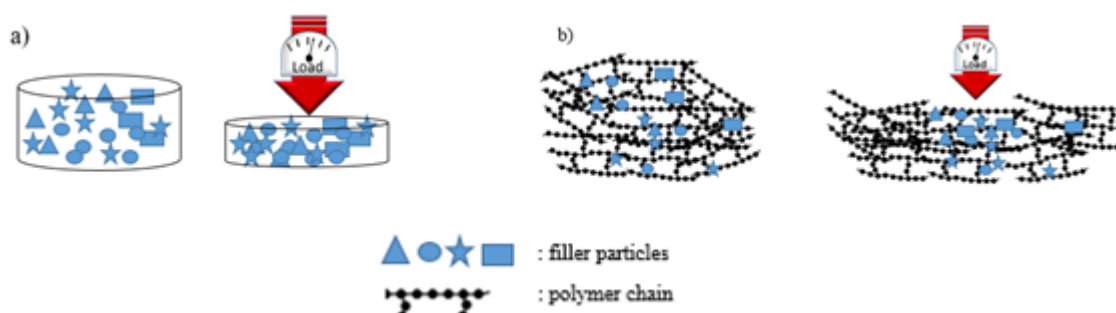


Figure 6: behaviour of a) powders and b) composite during compression

The resistance value, R , with the value of surface S and distance l between copper surfaces where used in Ohm law ($\rho=l/RS$) to evaluate the conductivity σ . Conductivity value of carbon powder and composite were evaluated following this procedure:

- 1) A starting value of conductivity was evaluated without any sample in order to measure the value of resistance of the system. This value was subtracted to the resistance value read with samples.
- 2) The same quantity of carbon powders (CB and Biochar) were positioned between copper cylinders and kept by Plexiglas hollow cylinder. The measurement was repeated several times in order to have a reliable value.
- 3) Composite was positioned between copper cylinders, in this case the Plexiglas hollow cylinder was not necessary and the value of conductivity was measured in different sample portions.

Preliminary results are reported in Figure 7 showing the conductivity of the biochar powders (red line) and percolation curves of related composites.

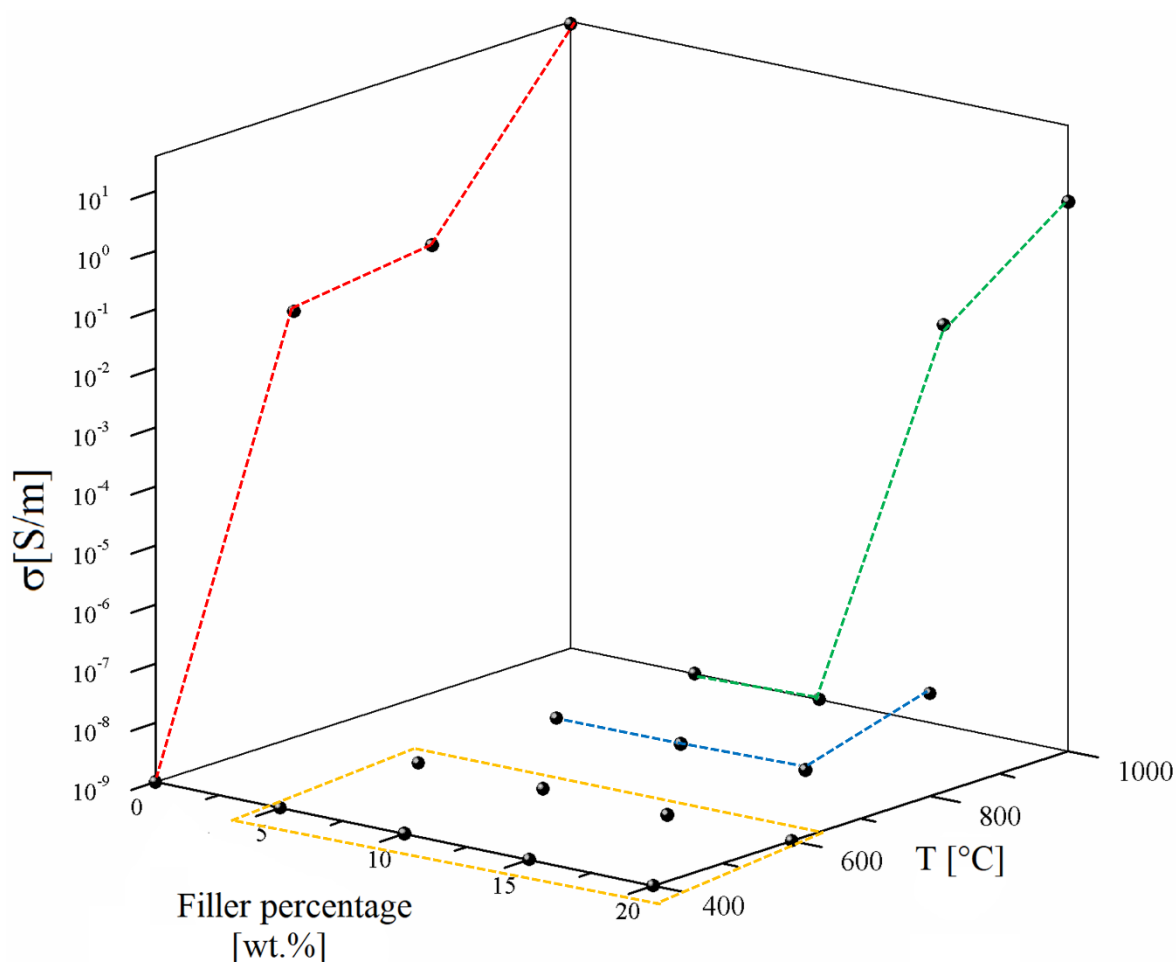


Figure 7: Trends of composites conductivity as function of filler percentage. Red line represents the biochar conductivity trends while yellow, blue and green show respectively the percolation curves of composites containing C400-C600, C800 and C1000.

C400 did not show an appreciable conductivity while an increment of pyrolytic temperature up to 600 °C induce a conductivity of up to 0.02 S/m. Further increments of processing temperature up to 800 °C and 1000 °C lead to a conductivity of up to 0.04 S/m and 35.96 S/m. This remarkable increment of conductivity between 800 °C and 1000 °C was due the enlargement of aromatic region formed as consequence of high temperature carbonization[44]. This deeply affected the electrical behaviour of related composites. Consequently, CB400 and CB600 containing composites were not conductive for all the range of filler percentage investigated. CB composites were not conductive until the filler

concentration of 15 wt.% reaching a conductivity of 5.4×10^{-8} S/m with a filler loading of 20 wt.%. CB100 composites showed the best performances showing a detectable electrical conductivity with a 15 wt.% of filler and reaching a conductivity of 2.02 S/m with a filler loading of 20 wt.%.

Accordingly with these data, electrical properties of CB1000 and CB1000 containing composites were studied under a wide range of static pressures comparing with the related CB and CB composites as shown in Figure 8.

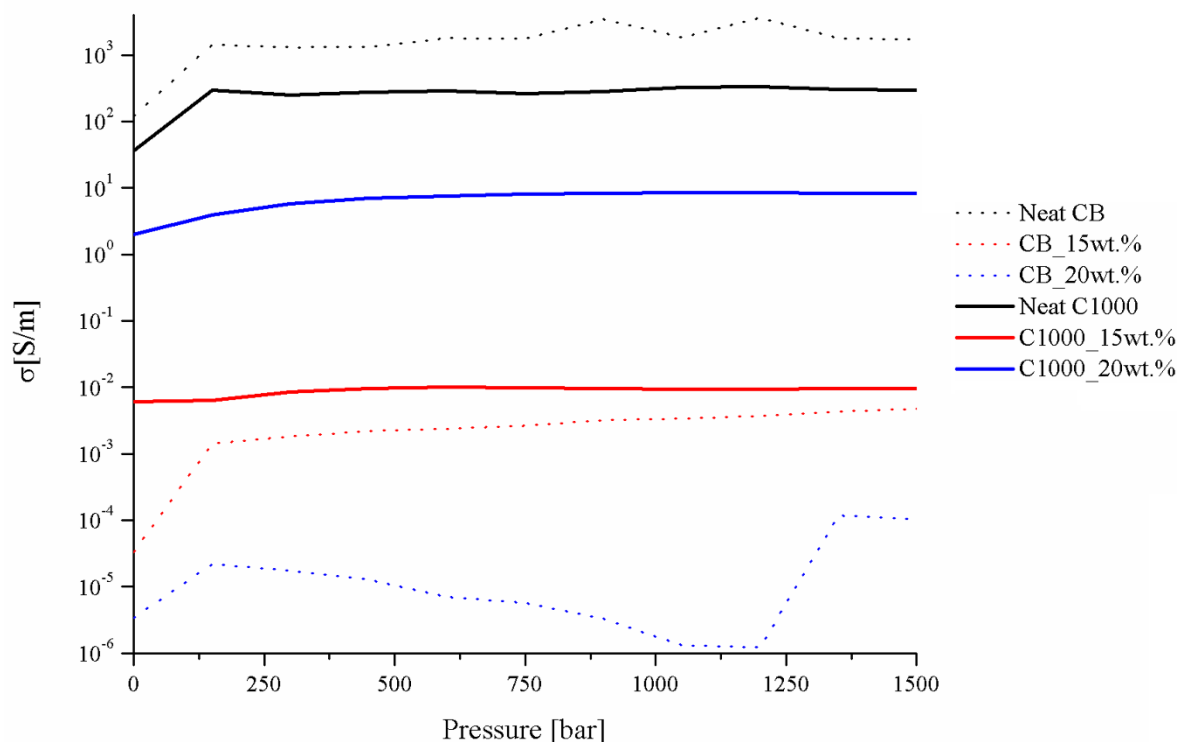


Figure 8: Trends of CB and C1000 powders and related composites conductivity as function of pressure applied.

CB powder reached a conductivity around 1700 S/m while in the same conditions C1000 reached a conductivity of 300 S/m. Composites containing of CB and C1000 were conductive but results showed a different trend compared with the relative powders. CB 15 wt.% reached the value of 4×10^{-3} S/m and its conductive value showed an influence of applied pressure in the first compression movement.. C1000 15 wt.% reached to 10^{-2} S/m, with an increment around four order of magnitude if compared with CB 15 wt.%. This difference was more relevant for a filler concentration of 20 wt.%. In this case, the conductivity of CB based composites drop down till 10^{-5} - 10^{-4} S/m while C1000 reached 8.38 S/m. High conductive value could be due to more uniform filler dispersion inside epoxy resin. Dispersion of the filler inside the epoxy matrix was investigated through FE-SEM (Figure 9) after samples cryo-fracture using liquid nitrogen compared composites with a filler loading of 15 wt.% due to the similarity of conductivity. CB containing composites showed dark and clear area (Figure 9a) with different compositions. The clear ones were rich in CB (Figure 9 b-c) meanwhile the darkest were poor (Figure 9 d). C1000 containing composites showed smooth surface with holes (Figure 9 e) due the expulsion of embedded C1000 particles during the fracturing (Figure 8 e) as clearly showed in Figure 8 g. Particles size analysis (Figure 10) showed clearly that C1000 was composed by two particles populations one around 100 μm and one around 20 μm . Considering the average size of C1000 particles into the composites is reasonably assume that the bigger ones underwent to a disruption during the ultrasonication forming small size well dispersed particles. Also, CB particles size showed that is more appropriated speaking of carbon black aggregates instead of single particles.

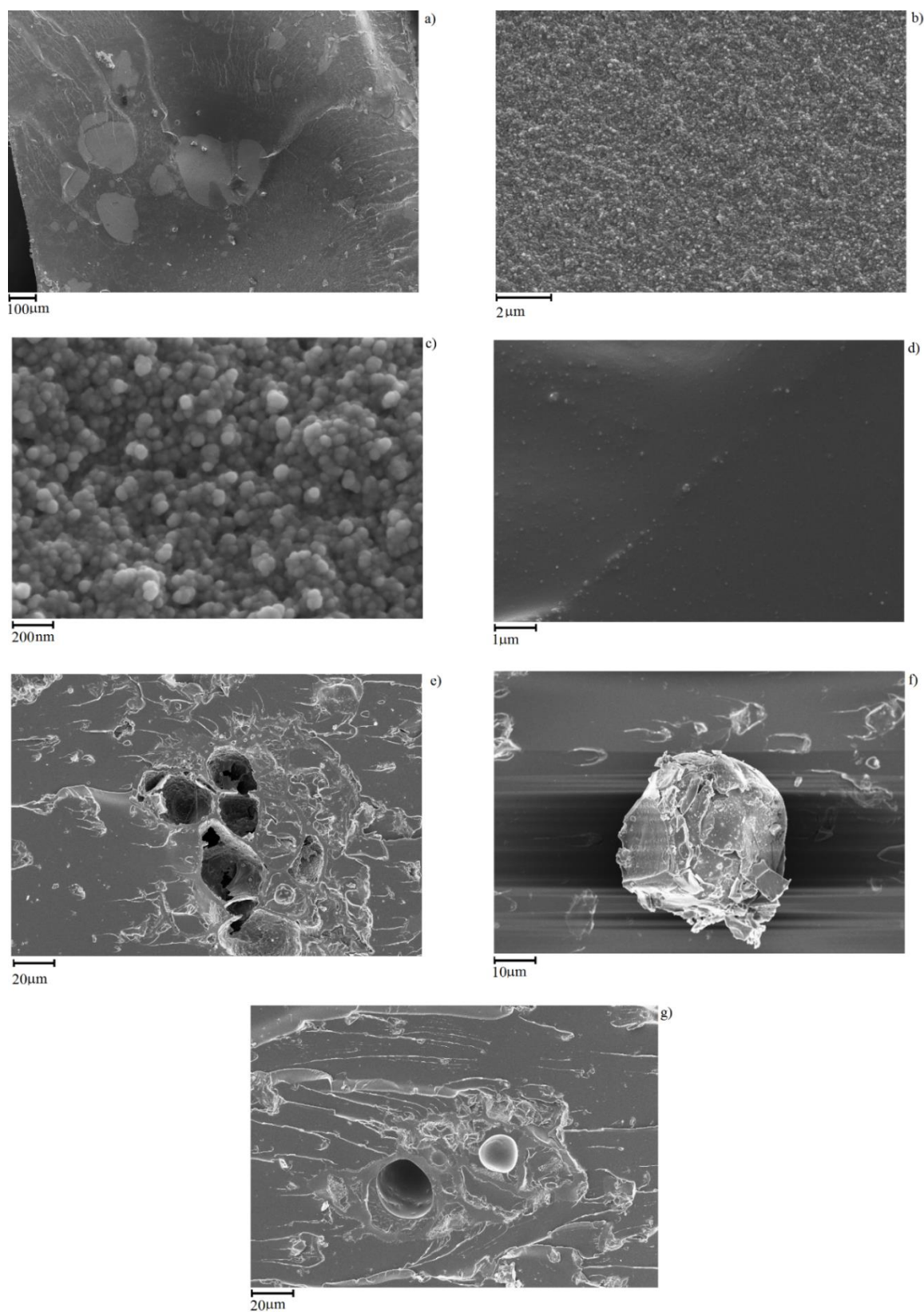


Figure 9: FESEM of cryo-fractured a-d) CB and e-g) C1000 containing composites with a filler loading of 15wt.%

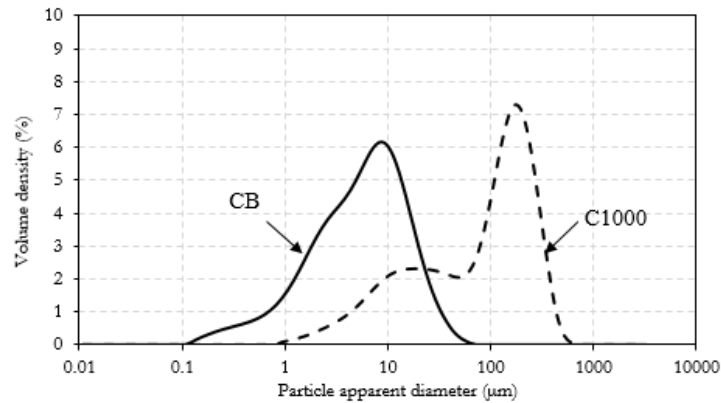


Figure 10: Particle size distribution for CB and C1000

3.2.2. Composite mechanical characterization

With the aim to confirm mechanical consistence of samples a stress-strain curve was investigate for composites of CB 15 wt.% and C1000 compared with neat resin. Mechanical tests on dog-bones shaped samples are summarized in the Figure 11.

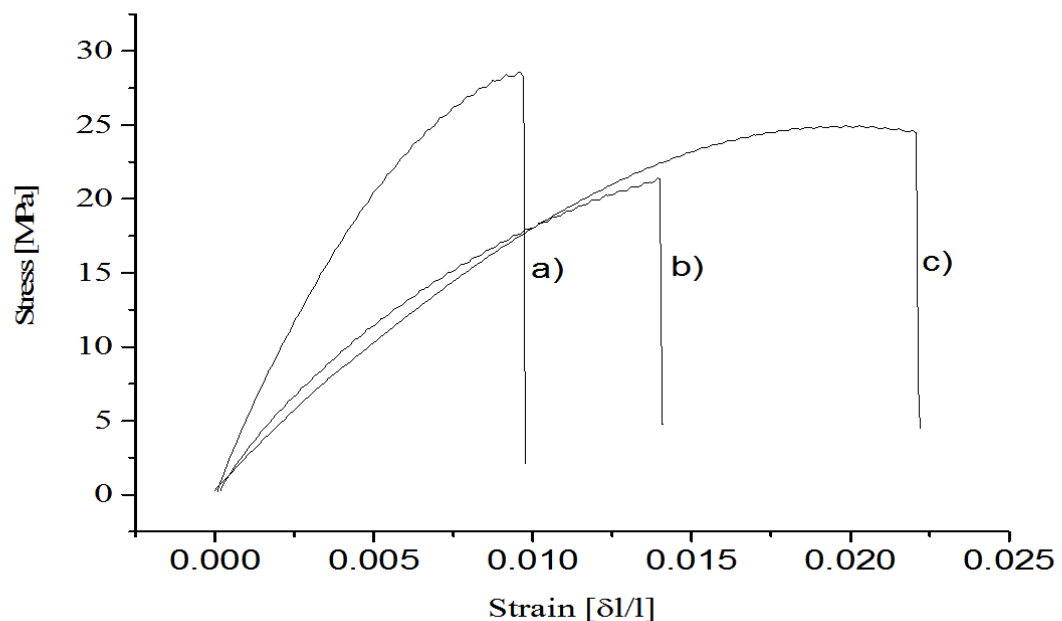


Figure 11: Stress-strain curves of composites containing 15 wt.% of a) C1000, b) CB and c) neat resin.

According to data report in Figure 12, maximum elongation of neat resin (3.50 ± 0.64 %) was the highest compared with those of C1000 and CB containing composites (1.16 ± 0.09 % and 1.63 ± 0.08 % respectively). Also, neat resin showed a remarkably higher toughness (0.48 ± 0.03 MJ/m³) compared with composites that showed values not significantly different from each other close to 0.18 MJ/m³. Young's modulus showed a significantly difference between C1000 based composites (3258 ± 273 MPa) and CB ones (1940 ± 163 MPa). These last values were quite close to those of neat resin (1510 ± 160 MPa) and a similar trend was observed with ultimate tensile strength with values of carbon black composites not significantly different from those of neat resin (both close to 19 MPa) and higher

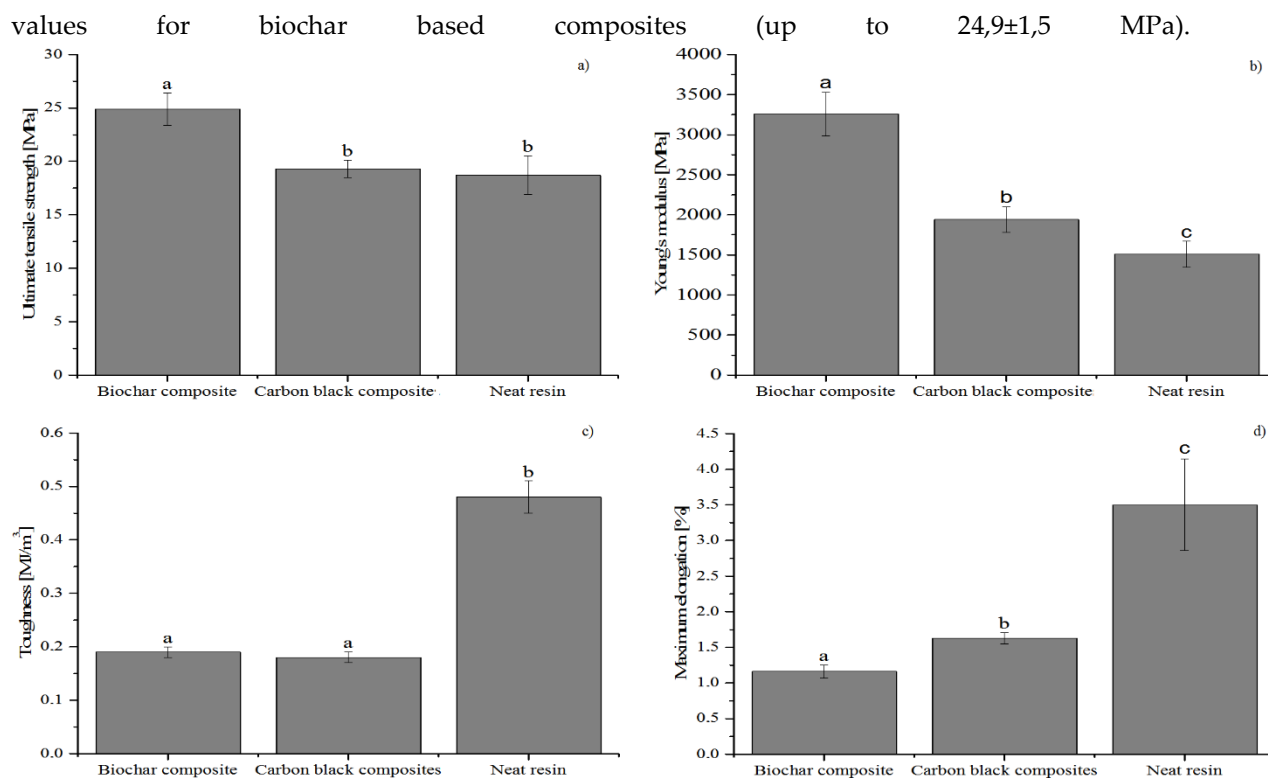


Figure 12: Summary of a) ultimate tensile strength, b) Young's modulus, c) toughness, d) maximum elongation of neat resin, biochar and carbon based composites. Columns marked with same letters are no significantly different ($p < 0.05$).

Composites behaviour observed during the mechanical tests enlighten the different interaction between different carbonaceous filler with epoxy matrix with magnification of filler-resin interaction in the case of biochar based composites with an increase brittleness and a reduced elongation.

4. Conclusions

Coffee waste stream was efficiently used as feedstock for pyrolytic conversion at different temperatures. The effect of process temperature on the properties of biochar was investigated and it was observed that further increments of temperature improved the porous stability and conductivity of the material.

Even if thermal treated biochar showed less conductivity respect to CB when it is dispersed in composite the electrical properties of composite containing coffee biochar are four order of magnitude higher than composite containing carbon black. Mechanical properties of composite with coffee biochar were verified and they are not compromises respect to composite containing carbon black.

Considering the sustainability of the biochar production, the results reported showed how carbon for biomasses could be a sound replacement for traditional carbon fillers as carbon black.

Acknowledgements: Authors acknowledge Andrea Marchisio for particle size analysis, Salvatore Guastella for FE-SEM and EDX analysis, Massimo Rovere for Raman spectra, Prof. Carlo Rosso for mechanical tests and Prof. Alberto Tagliaferro for fruitfully discussions.

Author Contributions: Conceptualization, M.G.; methodology M.G., M.B.; formal analysis M.G., M.B.; investigation M.G., M.B.; resources, M.G.; data curation, M.G., M.B.; writing—original draft preparation, M.G., M.B.; writing—review and editing, M.G., M.B.; supervision, M.G.

Funding: Acknowledgments: MODCOMP project (grant 685844, European H2020 program)

Conflicts of Interest: The authors declare no conflict of interest

References

1. Giroto, F.; Alibardi, L.; Cossu, R. Food waste generation and industrial uses: a review. *Waste management* **2015**, *45*, 32-41.
2. Burkhard, R.; Deletic, A.; Craig, A. Techniques for water and wastewater management: a review of techniques and their integration in planning. *Urban water* **2000**, *2*, 197-221.
3. Sängler, C. Value addition in the coffee sector. In Proceedings of 10th MULTI-YEAR EXPERT MEETING ON COMMODITIES AND DEVELOPMENT, Geneva.
4. Battista, F.; Fino, D.; Mancini, G. Optimization of biogas production from coffee production waste. *Bioresource technology* **2016**, *200*, 884-890.
5. Kusch, S.; Udenigwe, C.C.; Gottardo, M.; Micolucci, F.; Cavinato, C. First-and second-generation valorisation of wastes and residues occurring in the food supply chain. **2014**.
6. Sena da Fonseca, B.; Vilão, A.; Galhano, C.; Simão, J. Reusing coffee waste in manufacture of ceramics for construction. *Advances in Applied Ceramics* **2014**, *113*, 159-166.
7. Lafi, R.; ben Fradj, A.; Hafiane, A.; Hameed, B. Coffee waste as potential adsorbent for the removal of basic dyes from aqueous solution. *Korean Journal of Chemical Engineering* **2014**, *31*, 2198-2206.
8. Dominguez, A.; Menéndez, J.; Fernandez, Y.; Pis, J.; Nabais, J.V.; Carrott, P.; Carrott, M.R. Conventional and microwave induced pyrolysis of coffee hulls for the production of a hydrogen rich fuel gas. *Journal of Analytical and Applied Pyrolysis* **2007**, *79*, 128-135.
9. Tsai, W.-T.; Liu, S.-C.; Hsieh, C.-H. Preparation and fuel properties of biochars from the pyrolysis of exhausted coffee residue. *Journal of Analytical and Applied Pyrolysis* **2012**, *93*, 63-67.
10. Qian, K.; Kumar, A.; Zhang, H.; Bellmer, D.; Huhnke, R. Recent advances in utilization of biochar. *Renewable and Sustainable Energy Reviews* **2015**, *42*, 1055-1064.
11. Ok, Y.S.; Chang, S.X.; Gao, B.; Chung, H.-J. SMART biochar technology—a shifting paradigm towards advanced materials and healthcare research. *Environmental Technology & Innovation* **2015**, *4*, 206-209.
12. Ziegler, D.; Palmero, P.; Giorcelli, M.; Tagliaferro, A.; Tulliani, J.-M. Biochars as Innovative Humidity Sensing Materials. *Chemosensors* **2017**, *5*, 35.
13. Jiang, J.; Zhang, L.; Wang, X.; Holm, N.; Rajagopalan, K.; Chen, F.; Ma, S. Highly ordered macroporous woody biochar with ultra-high carbon content as supercapacitor electrodes. *Electrochimica Acta* **2013**, *113*, 481-489.
14. Khan, A.; Jagdale, P.; Rovere, M.; Nogués, M.; Rosso, C.; Tagliaferro, A. Carbon from waste source: An eco-friendly way for strengthening polymer composites. *Composites Part B: Engineering* **2018**, *132*, 87-96.
15. Arrigo, R.; Jagdale, P.; Bartoli, M.; Tagliaferro, A.; Malucelli, G. Structure–Property Relationships in Polyethylene-Based Composites Filled with Biochar Derived from Waste Coffee Grounds. *Polymers* **2019**, *11*, 1336.
16. Bartoli, M.; Giorcelli, M.; Rosso, C.; Rovere, M.; Jagdale, P.; Tagliaferro, A. Influence of Commercial Biochar Fillers on Brittleness/Ductility of Epoxy Resin Composites. *Applied Sciences* **2019**, *9*, 3109.
17. Association, I.C.B. What is Carbon Black? Available online: <http://www.carbon-black.org/> (accessed on
18. Tchoudakov, R.; Breuer, O.; Narkis, M.; Siegmann, A. Conductive polymer blends with low carbon black loading: polypropylene/polyamide. *Polymer Engineering & Science* **1996**, *36*, 1336-1346.
19. Quosai, P.; Anstey, A.; Mohanty, A.K.; Misra, M. Characterization of biocarbon generated by high-and low-temperature pyrolysis of soy hulls and coffee chaff: for polymer composite applications. *Royal Society open science* **2018**, *5*, 171970.

20. Field, J.L.; Keske, C.M.; Birch, G.L.; DeFoort, M.W.; Cotrufo, M.F. Distributed biochar and bioenergy coproduction: a regionally specific case study of environmental benefits and economic impacts. *Gcb Bioenergy* **2013**, *5*, 177-191.
21. Dutta, B.; Raghavan, V. A life cycle assessment of environmental and economic balance of biochar systems in Quebec. *International Journal of Energy and Environmental Engineering* **2014**, *5*, 106.
22. Roberts, K.G.; Gloy, B.A.; Joseph, S.; Scott, N.R.; Lehmann, J. Life cycle assessment of biochar systems: estimating the energetic, economic, and climate change potential. *Environmental science & technology* **2009**, *44*, 827-833.
23. Liang-Hsing, L.; Lin, Y.-j.; Lin, Y.-s.; Hwang, K.-Y.; Yi-Sern, W. Reactive epoxy compounds and method for producing the same, core-shell type epoxy resin particles, waterborne epoxy resin composition, and coating composition containing the reactive epoxy compounds. Google Patents: 2019.
24. Ahmadi, Z. Nanostructured epoxy adhesives: a review. *Progress in Organic Coatings* **2019**, *135*, 449-453.
25. Liao, J.; Zhang, D.; Wu, X.; Luo, H.; Zhou, K.; Su, B. Preparation of high strength zirconia by epoxy gel-casting using hydantion epoxy resin as a gelling agent. *Materials Science and Engineering: C* **2019**, *96*, 280-285.
26. Lall, P.; Dornala, K.; Deep, J.; Lowe, R. Measurement and Prediction of Interface Crack Growth at the PCB-Epoxy Interfaces Under High-G Mechanical Shock. In Proceedings of 2018 17th IEEE Intersociety Conference on Thermal and Thermomechanical Phenomena in Electronic Systems (ITherm); pp. 1097-1105.
27. Rana, S.; Alagirusamy, R.; Joshi, M. A review on carbon epoxy nanocomposites. *Journal of Reinforced Plastics and Composites* **2009**, *28*, 461-487.
28. Sela, N.; Ishai, O. Interlaminar fracture toughness and toughening of laminated composite materials: a review. *Composites* **1989**, *20*, 423-435.
29. Enhua, H.; Kaichang, K.; Lixin, C. Research Progress on Encapsulating Materials of Epoxy Resin. *Chemical Industry and Engineering Progress* **2003**, *22*, 1057-1060.
30. Jin, F.-L.; Li, X.; Park, S.-J. Synthesis and application of epoxy resins: A review. *Journal of Industrial and Engineering Chemistry* **2015**, *29*, 1-11.
31. Rafique, I.; Kausar, A.; Anwar, Z.; Muhammad, B. Exploration of epoxy resins, hardening systems, and epoxy/carbon nanotube composite designed for high performance materials: a review. *Polymer-Plastics Technology and Engineering* **2016**, *55*, 312-333.
32. Wajid, A.S.; Ahmed, H.T.; Das, S.; Irin, F.; Jankowski, A.F.; Green, M.J. High-Performance Pristine Graphene/Epoxy Composites With Enhanced Mechanical and Electrical Properties. *Macromolecular Materials and Engineering* **2013**, *298*, 339-347.
33. Wang, F.; Drzal, L.T.; Qin, Y.; Huang, Z. Mechanical properties and thermal conductivity of graphene nanoplatelet/epoxy composites. *Journal of materials science* **2015**, *50*, 1082-1093.
34. Gojny, F.H.; Wichmann, M.H.; Fiedler, B.; Schulte, K. Influence of different carbon nanotubes on the mechanical properties of epoxy matrix composites—a comparative study. *Composites Science and Technology* **2005**, *65*, 2300-2313.
35. Sandler, J.; Shaffer, M.; Prasse, T.; Bauhofer, W.; Schulte, K.; Windle, A. Development of a dispersion process for carbon nanotubes in an epoxy matrix and the resulting electrical properties. *Polymer* **1999**, *40*, 5967-5971.
36. Tubes, C. Welcome To Cheap Tubes. Available online: <https://www.cheaptubes.com/> (accessed on 09 October 2019).

37. Smail, F.; Boies, A.; Windle, A. Direct spinning of CNT fibres: Past, present and future scale up. *Carbon* **2019**, *152*, 218-232, doi:<https://doi.org/10.1016/j.carbon.2019.05.024>.
38. Medalia, A.I.; Rivin, D. Particulate carbon and other components of soot and carbon black. *Carbon* **1982**, *20*, 481-492.
39. Kambo, H.S.; Dutta, A. A comparative review of biochar and hydrochar in terms of production, physico-chemical properties and applications. *Renewable and Sustainable Energy Reviews* **2015**, *45*, 359-378, doi:<https://doi.org/10.1016/j.rser.2015.01.050>.
40. Weber, K.; Quicker, P. Properties of biochar. *Fuel* **2018**, *217*, 240-261.
41. Ferrari, A.C.; Robertson, J. Interpretation of Raman spectra of disordered and amorphous carbon. *Physical review B* **2000**, *61*, 14095.
42. Bishui, B. On the Origin of Fluorescence in Diamond. **1950**.
43. Oberlin, A. Carbonization and graphitization. *Carbon* **1984**, *22*, 521-541.
44. De Fonton, S.; Oberlin, A.; Inagaki, M. Characterization by electron microscopy of carbon phases (intermediate turbostratic phase and graphite) in hard carbons when heat-treated under pressure. *Journal of Materials Science* **1980**, *15*, 909-917.